The Plant Cell, Vol. 17, 2676–2692, October 2005, www.plantcell.org © 2005 American Society of Plant Biologists

The Tomato *Aux/IAA* Transcription Factor *IAA9* Is Involved in Fruit Development and Leaf Morphogenesis [W]

Hua Wang,[a] Brian Jones,[a] Zhengguo Li,[b] Pierre Frasse,[a] Corinne Delalande,[a] Farid Regad,[a] Salma Chaabouni,[a] Alain Latché,[a] Jean-Claude Pech,[a] and Mondher Bouzayen[a,1]

[a] Unité Mixte de Recherche 990, Institut National de la Recherche Agronomique/Institut National Polytechnique–Ecole Nationale Supérieure Agronomique Toulouse, Génomique et Biotechnologie des Fruits Pôle de Biotechnologie Végétale, 31326 Castanet-Tolosan Cedex, France

[b] Genetic Engineering Research Center, Chongqing University, 40030 Chongqing, China

Auxin/indole-3-acetic acid (Aux/IAA) proteins are transcriptional regulators that mediate many aspects of plant responses to auxin. While functions of most Aux/IAAs have been defined mainly by gain-of-function mutant alleles in *Arabidopsis thaliana*, phenotypes associated with loss-of-function mutations have been scarce and subtle. We report here that the downregulation of *IAA9*, a tomato (*Solanum lycopersicum*) gene from a distinct subfamily of *Aux/IAA* genes, results in a pleiotropic phenotype, consistent with its ubiquitous expression pattern. *IAA9*-inhibited lines have simple leaves instead of wild-type compound leaves, and fruit development is triggered before fertilization, giving rise to parthenocarpy. This indicates that IAA9 is a key mediator of leaf morphogenesis and fruit set. In addition, antisense plants displayed auxin-related growth alterations, including enhanced hypocotyl/stem elongation, increased leaf vascularization, and reduced apical dominance. Auxin dose–response assays revealed that *IAA9* downregulated lines were hypersensitive to auxin, although the only early auxin-responsive gene that was found to be upregulated in the antisense lines was *IAA3*. The activity of the *IAA3* promoter was stimulated in the *IAA9* antisense genetic background, indicating that IAA9 acts in planta as a transcriptional repressor of auxin signaling. While no mutation in any member of subfamily IV has been reported to date, the phenotypes associated with the downregulation of *IAA9* reveal distinct and novel roles for members of the *Aux/IAA* gene family.

INTRODUCTION

The phytohormone auxin is central to a myriad of aspects of plant growth and developmental processes. At the cellular level, auxin controls cell division, extension, and differentiation. On a whole-plant level, auxin plays an essential role in processes such as apical dominance, lateral/adventitious root formation, tropisms, fruit set and development, vascular differentiation, and embryogenesis (Friml, 2003). While it is clear that auxin plays a pivotal role in plant growth and development, the molecular effectors by which this hormone exerts its effect are still relatively unknown. For example, in the process of fruit set, the onset of ovary development into fruit and its subsequent development are naturally triggered by signals from successful fertilization. These processes can be initiated in the absence of pollination and fertilization by exogenous auxin or auxin transport inhibitors (Gustafson, 1937; Beyer and Quebedeaux, 1974) or by the ovary-specific expression of *Agrobacterium tumefaciens indoleacetamide monoxygenase* (*iaaM*) or *root loci B* (*rolB*) genes, which confer higher auxin production or increased auxin sensitivity, respectively (Ficcadenti et al., 1999; Carmi et al., 2003). The molecular mediators by which auxin impacts this process are still unknown.

The recent discovery that the F-box protein Transport Inhibitor Response1 functions as an auxin receptor represents a major breakthrough (Dharmasiri et al., 2005; Kepinski and Leyser, 2005) in understanding how auxin mediates cellular responses. It has been known for a decade that auxin signaling operates by recruiting specific transcription factors, leading to the expression of downstream genes that perform the required responses (Vogler and Kuhlemeier, 2003). The auxin/indole-3-acetic acid (Aux/IAA) and auxin response factor (ARF) families of transcription factors have been shown to be instrumental in auxin-dependent transcriptional regulation. Aux/IAA proteins are short-lived transcription factors that share four highly conserved domains. Domain I contains a functionally characterized transcriptional repressor motif (Tiwari et al., 2004), while domain II interacts with a component of the ubiquitin-proteasome protein degradation pathway shown to be essential for auxin signaling. Domains III and IV act as C-terminal dimerization domains, mediating homodimerization and heterodimerization among Aux/IAA family members and dimerization with similar domains found in ARFs (Kim et al., 1997; Ulmasov et al., 1997; Ouellet et al., 2001). ARFs are transcriptional activators and repressors that bind with specificity to TGTCTC auxin-responsive *cis*-acting elements found in promoters of primary/early auxin-responsive genes, including members of the *Aux/IAA* family (Ulmasov et al., 1997).

Aux/IAA genes are expressed in distinct spatial and temporal patterns, contributing to the diversity of auxin responses in different plant tissues, organs, and developmental stages (Abel et al.,

[1] To whom correspondence should be addressed. E-mail bouzayen@ensat.fr; fax 0033-5-62193573.
The author responsible for distribution of materials integral to the findings presented in this article in accordance with the policy described in the Instructions for Authors (www.plantcell.org) is: Mondher Bouzayen (bouzayen@ensat.fr).

[W] Online version contains Web-only data.

Article, publication date, and citation information can be found at www.plantcell.org/cgi/doi/10.1105/tpc.105.033415.

1995). Screens for *Arabidopsis thaliana* mutants with altered auxin response or morphology have identified mutations in 10 different *Aux/IAA* genes: *IAA1/AXR5* (Park et al., 2002; Yang et al., 2004), *IAA3/SHY2* (Tian and Reed, 1999), *IAA6/SHY1* (Kim et al., 1996), *IAA7/AXR2* (Nagpal et al., 2000), *IAA12/BDL* (Hamann et al., 2002), *IAA14/SLR* (Fukaki et al., 2002), *IAA17/AXR3* (Rouse et al., 1998), *IAA18* (Reed, 2001), *IAA19/MSG2* (Tatematsu et al., 2004), and *IAA28* (Rogg et al., 2001). All of these primary mutations in *Aux/IAA* genes were found in the highly conserved domain II, which is responsible for protein degradation. The mutations stabilize the proteins, resulting in gain-of-function phenotypes. Several revertants have been shown to have mutations in other domains, affecting the capacity of the hyperstable proteins to function (Rouse et al., 1998). The *aux/iaa* mutants exhibit a variety of auxin-related developmental phenotypes, including altered phototropism/gravitropism, root formation, apical dominance, stem/hypocotyl elongation, leaf expansion, and leaf formation in the dark. However, because the stabilization caused by these mutations may not mimic regulatory events actually occurring in wild-type plants, accurate determination of the physiological significance of Aux/IAA proteins would benefit from the study of loss-of-function mutants. Unfortunately, the few *Aux/IAA* null mutations that have been characterized display subtle or nonscorable phenotypes, probably due to functional redundancy or to feedback regulatory loops that enable the mutant plants to compensate for absence of a particular Aux/IAA protein.

We report here on the functional characterization of *IAA9*, a member of subfamily IV of the tomato (*Solanum lycopersicum*) *Aux/IAA* gene family for which, to our knowledge, no mutation has been described so far. Phenotypes and molecular analyses of the downregulation of *IAA9* in transgenic tomatoes indicated that the IAA9 protein is a pivotal mediator of auxin in the process of fruit set and leaf morphogenesis. The evidence provided by this work supports the hypothesis that the IAA9 protein acts to repress the auxin response pathway.

RESULTS

IAA9 Belongs to a Distinct Subfamily of the *Aux/IAA* Gene Family

IAA9 and other partial tomato *Aux/IAA* clones were isolated from tomato fruit using gene family–specific degenerate primers designed to conserve sequences in *Aux/IAA*s from different plant species (Jones et al., 2002). The *IAA9* cDNA clone was found to correspond to a previously isolated 301-bp partial tomato clone (Nebenfuhr et al., 2000), initially named *IAA4* (GenBank accession number AF022015). The complete coding sequence (1047 bases), encoding a putative protein of 349 amino acids, was then isolated and renamed *IAA9* to comply with the numbering retained for the *Arabidopsis Aux/IAA* genes. The derived protein comprises the four conserved domains characteristic of the *Aux/IAA* gene family, domains I to IV, and several nuclear localization signal (NLS) sequences (Figure 1). Phylogenetic analysis was conducted to assess the relationships between tomato *IAA9* and *Aux/IAA* genes from *Arabidopsis* and other plant species. The phylogenetic tree shown in Figure 2 suggests that *Aux/IAA* proteins can be grouped into four subfamilies. Subfamilies II, III, and IV are well defined, and their existence was confirmed by both PAUP and ProDom analyses (Servant et al., 2002). Subfamily I includes up to six subgroups, each of them bearing at least one specific domain. Tomato IAA9 falls into subfamily IV along with sequences from grape (*Vitis vinifera*), cucumber (*Cucumis sativus*), *Zinnia elegans*, and *Arabidopsis*. Three other tomato Aux/IAA proteins, highly similar to their putative *Arabidopsis* homologs, fall into three of the four main subfamilies. Subfamily IV is clearly distinguishable from other Aux/IAA subfamilies, as its members are longer (typically >300 amino acids) than members of all other subfamilies (~200 amino acids) and typically contain 40 to 60 additional amino acids N-terminal to domain I and >50 amino acids between domains I and II (Figure 1). This N-terminal region unique to subfamily IV is well conserved among different plant species (shaded in gray in Figure 1), which suggests conserved function. The predicted tomato IAA9 protein shares 97% identity with potato (*Solanum tuberosum*) Aux/IAA and 92% similarity with tobacco (*Nicotiana tabacum*) IAA9. It also shares 80, 78, 74, and 70% similarity with grape Aux/IAA, cucumber IAA2, *Z. elegans* auxin-responsive protein (ARP), and *Arabidopsis* IAA9, respectively. Tomato IAA9 contains several highly conserved amino acid sequence motifs (Figure 1) unique to subfamily IV such as the short $(Pxx)_2$ sequences located between domains I and II, which are indicative of polyproline II conformations.

The predicted bipartite NLS comprised an invariant basic doublet KR in interdomain I/II and basic amino acids in domain II. A second SV40-type NLS is located in domain IV (Figure 1). The nuclear localization of the IAA9 protein was investigated by fusion to the green fluorescent protein (GFP) under the control of the 35S promoter of *Cauliflower mosaic virus* and transient expression in tobacco protoplasts. Fluorescence microscopy analysis associated with image overlay techniques demonstrated that control cells transformed with GFP alone displayed fluorescence throughout the cell (Figure 3), whereas the IAA9-GFP fusion protein was exclusively localized to the nucleus, indicating that IAA9 was able to fully direct the fusion protein to the nucleus (Figure 3). This nuclear targeting of the IAA9 protein is consistent with a putative transcriptional regulatory function.

IAA9 Expression Is Ubiquitous and Constitutive

RT-PCR analyses showed that basal expression of the *IAA9* gene was high in roots, stems, leaves, flowers, and fruit (Figure 4A). Expression data gained from The Institute for Genomic Research tomato EST database (http://www.tigr.org/tdb/tgi/lgi) and the Solanaceae Genome Network tomato expression database (http://www.sgn.cornell.edu) indicated that *IAA9* is also highly expressed in seeds and in vitro–cultured callus tissues. The low number of cycles (<22) required for successful RT-PCR amplification in all tomato tissues examined suggested that the basal transcript levels for *IAA9* were higher than for other tomato *Aux/IAA*s (H. Wang and M. Bouzayen, unpublished data). *IAA9* expression also showed constitutive expression throughout leaf and fruit ontogeny (Figures 4B and 4C). In contrast with the majority of *Aux/IAA* gene family members, including *IAA2*, *IAA3*, and *IAA8*, that show rapid and strong induction by auxin,

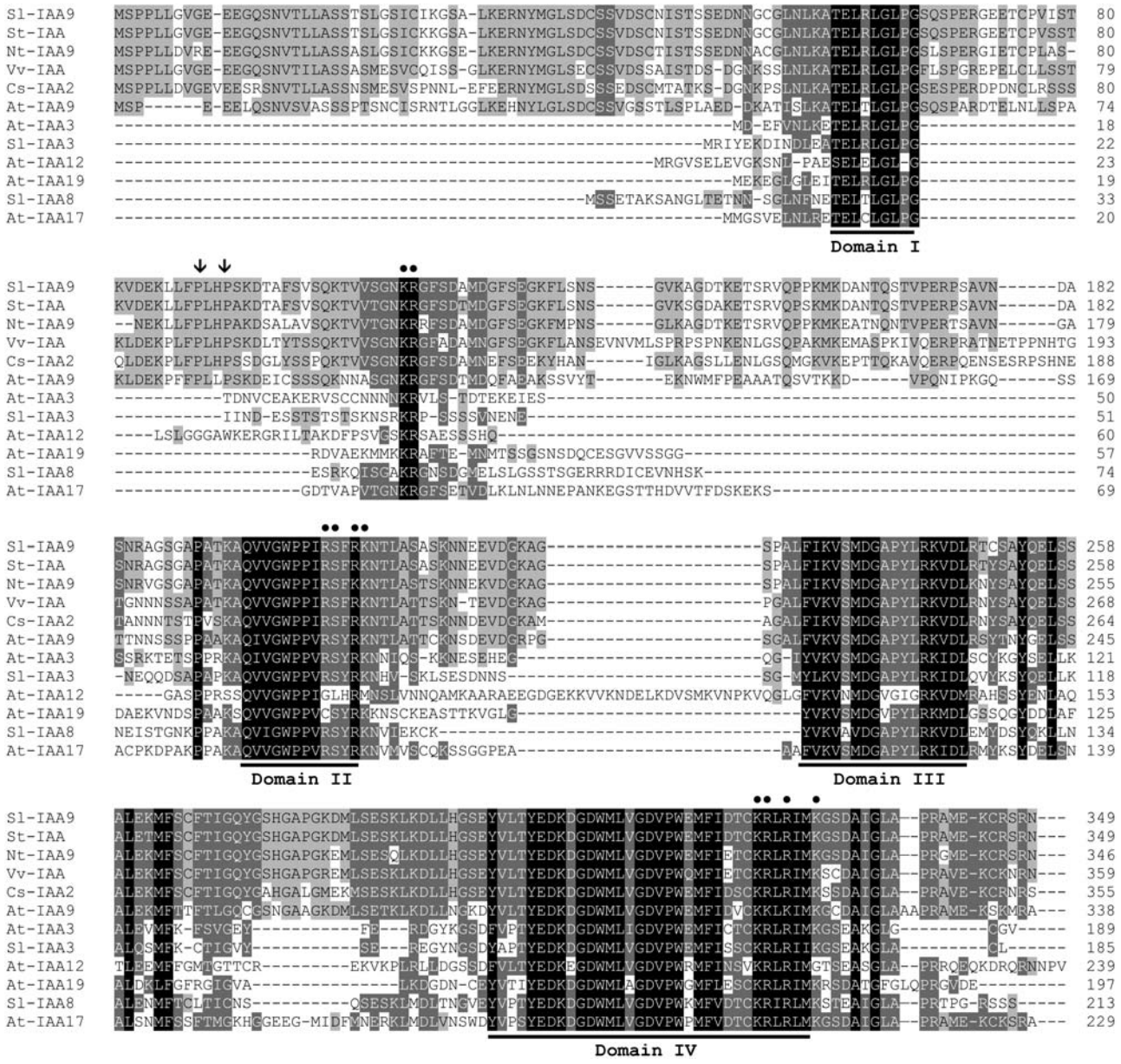

Figure 1. Sequence Analysis of IAA9.

Sequence comparison of IAA9, putative orthologs from other plants, and other members of the Aux/IAA protein family. Conserved residues are shaded in black, dark gray shading indicates similar residues in at least 7 out of 12 of the sequences, and light gray shading indicates similar residues in 4 to 6 out of 12 of the sequences. The four conserved domains I, II, III, and IV are underlined. Conserved basic residues that putatively function as NLS are indicated by closed circles on the top of the alignment. Putative polyproline II $(Pxx)_2$ conformation residues are indicated by arrows.

IAA9 mRNA levels did not alter markedly after 30 min of auxin treatment, but increased after 3 h (Figure 4D).

IAA9 Antisense Plants Exhibited Altered Leaf Morphology and Multiple Organ Fusion

No mutants altered in the expression of subfamily IV members of the *Aux/IAA* gene family have been described to date. Therefore, an antisense construct of the *IAA9* gene was stably transformed into tomato plants to address the physiological significance of the encoded protein. Several transgenic antisense lines (*AS-IAA9*) corresponding to independent transformation events were selected and analyzed. *AS-IAA9* lines exhibited a wide range of phenotypic effects, suggesting an important role for IAA9 in a number of developmental processes. The most readily visible phenotype was related to leaf morphology. Wild-type tomato leaves are unipinnately compound with a terminal leaflet and three pairs of lobed major lateral leaflets with pinnate venation.

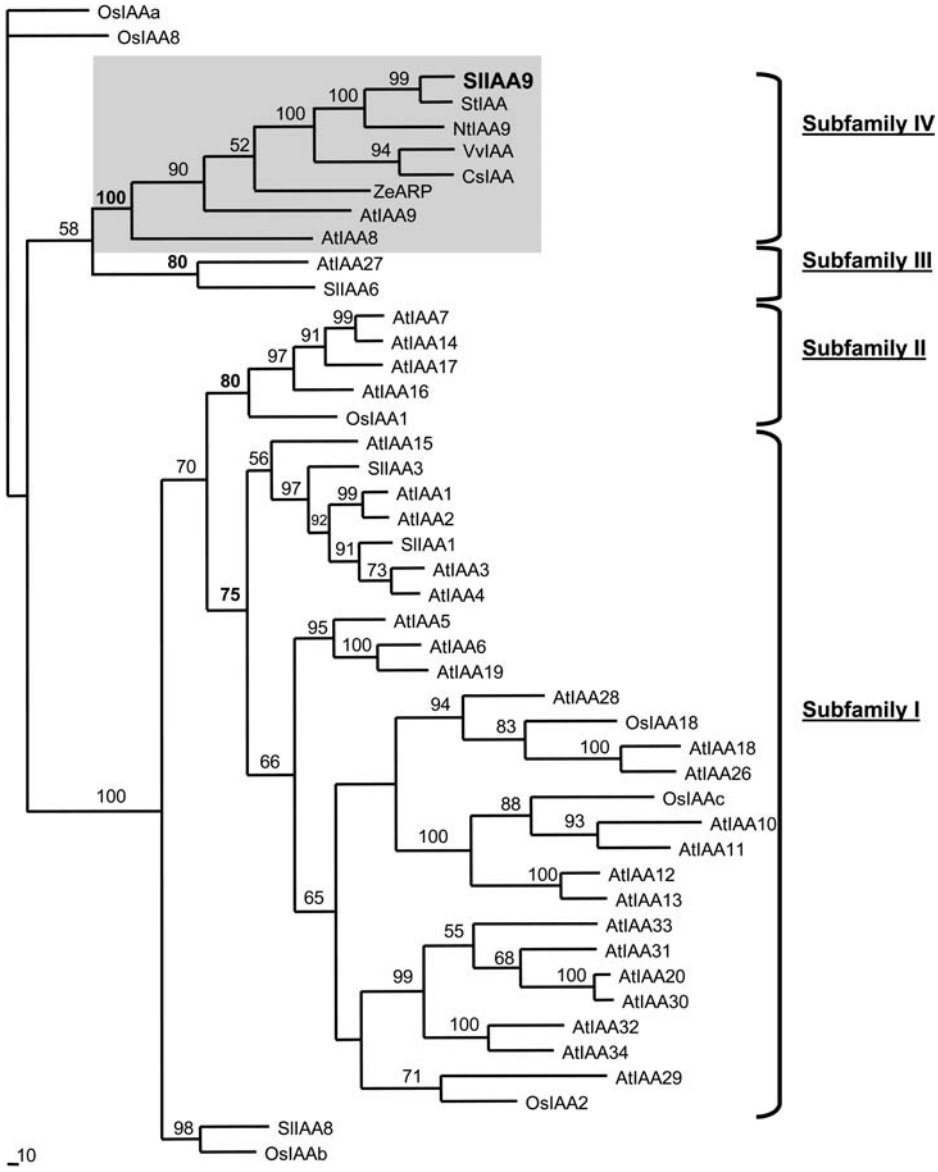

Figure 2. *IAA9* and Its Homologs Belong to a Distinct Subfamily of the *Aux/IAA* Gene Family.

The resultant tree was obtained by a character state cladistic approach (Parsimony) using OsIAAa and OsIAA8 as the outgroups (chosen because of their relative isolation on preliminary calculations). Values above branches are bootstrap percentages (5000 replicates). The score of the best tree found was 4442 with consistency index of 0.6376 and homoplasy index of 0.3624.

Smaller leaflets are often seen between the major leaflets (Figure 5A). By contrast, the leaves of *AS-IAA9* plants were characterized by minimally lobed simple leaves varying from perfect entire-margined simple leaves to compound leaves (Figure 5B) depending on the level of downregulation displayed by the different transgenic lines (Figures 5B and 5C). In the lobed simple leaves, one or more pair of lateral leaflets merges with the terminal leaflet. In these leaves, the borders between the leaflets often remain defined, and the lamina was frequently asymmetrical and wrinkled. The consistency of the phenotypes was supported by reproducing them in two different tomato genetic backgrounds: *MicroTom* and *Ailsa Craig* (Figures 5A and 5B).

The levels of *IAA9* transcripts were significantly reduced in five antisense transgenic lines compared with that of wild-type control plants (Figure 5C), further supporting that downregulation of *IAA9* accounts for the phenotypes displayed by the transgenic lines. *AS111* and *AS213* showed the strongest downregulation of *IAA9* and correspondingly were found to have the most severe phenotypes producing almost complete simple leaf morphology (Figures 5B and 5C). Lines *AS250* and *AS58* showed a less dramatic decrease in *IAA9* transcript accumulation and exhibited only moderate phenotypes with both simple and lobed simple leaves, whereas line *AS70* showed a slight decrease in *IAA9* transcript accumulation and a concomitant weak phenotype with

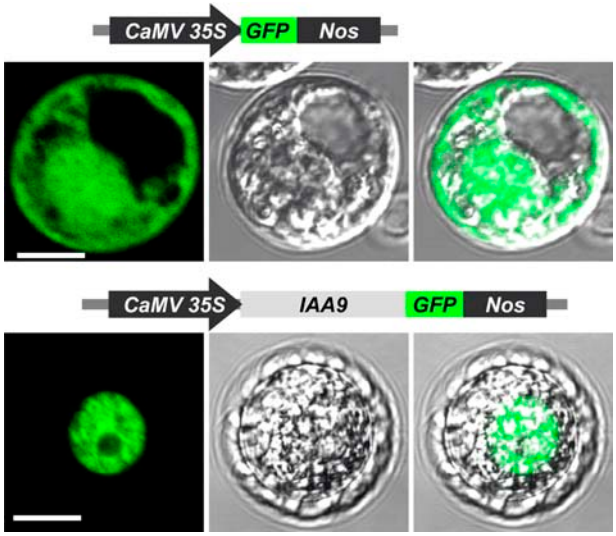

Figure 3. Nuclear Localization of the IAA9 Protein Fused to a GFP Tag.

Tobacco protoplasts were transiently transformed with either Pro$_{35S}$:*GFP* or Pro$_{35S}$:*IAA9-GFP* constructs, and the subcellular localizations of the IAA9-GFP fusion protein or the GFP were analyzed by confocal laser scanning microscopy (left panel). Light micrographs (middle panel) and fluorescence (left panel) images are merged (right panel) to illustrate the different location of the two proteins. Bars = 10 μm. CaMV, *Cauliflower mosaic virus*.

only occasional lobed simple leaves. Finally, line *AS252* showed a similar level of *IAA9* transcript accumulation to the wild type and was morphologically indistinguishable from wild-type plants. Interestingly, the phenotypes of *AS-IAA9* lines were reminiscent of simple leaves in the recessive spontaneous tomato mutant *entire*, which was also found to accumulate significantly lower levels of *IAA9* mRNA than wild-type plants (Figures 5A and 5C). By contrast, the expression of *IAA9* was not altered in *Lanceolate* and *Petroselinum*, two other leaf-shape mutants (see Supplemental Figure 1 online). Transcript accumulation of *KNOX* genes (*TKN1* and Le*T6*/*TKN2*) and *PHANTASTICA*, the ortholog of *Arabidopsis ASYMMETRIC LEAVES1*, all known to be involved in leaf morphogenesis (Kessler and Sinha, 2004), was not affected in whole expanding leaves, fruit, and seedlings of *AS-IAA9* lines (see Supplemental Figure 2 online).

AS-IAA9 lines also displayed multiple organ fusions. The majority of the fused petioles/leaves (Figure 5D) were position dependent and usually found between the first and the third true leaves that correspond to the transition leaves. Such a phenotype is reminiscent of the *Arabidopsis pin1* mutant affected in auxin transport (Galweiler et al., 1998). Fusions of flowers, fruit, cotyledons, and stems were also observed (see Supplemental Figure 3 online). In addition, bifurcated, triple, or quadruple cotyledons were also frequently observed in *AS-IAA9* seedlings (Figure 5E). While wild-type tomato flowers and fruit normally carry five to six symmetrically arranged sepals, *AS-IAA9* tomato invariably had partially fused and asymmetrically arranged sepals (Figure 5F). The tomato *entire* mutant also carries, though at a lower frequency, asymmetrical sepals and a multifusion phenotype affecting leaves, flowers, and fruits.

Fruit Set Prior to Pollination Results in Parthenocarpy in *AS-IAA9* Plants

Downregulation of *IAA9* resulted in a dramatic alteration of early fruit development, with all *AS-IAA9* lines exhibiting precocious fruit set prior to anthesis, resulting in parallel fruit and flower development (Figure 6B). Depending on how early the precocious enlargement of the fruit occurred, the development of the stamens was either completely impaired (Figure 6A), or in less severe cases, the fused stamen cones were torn open by the developing fruit (Figure 6B). The accelerated enlargement of the fruit positioned the stigma out of reach of the stamens, impairing self-pollination and contributing to the development of seedless fruit (Figure 6C). Despite their parthenocarpic character, these fruit were similar in appearance to wild-type tomato in terms of size, skin color, and flesh consistency (Figure 6C) as well as ripening-associated ethylene production (see Supplemental Figure 4 online). In the strongly inhibited line *AS111*, the proportion of parthenocarpic fruit reached 82% (Figure 6D). Once again, the

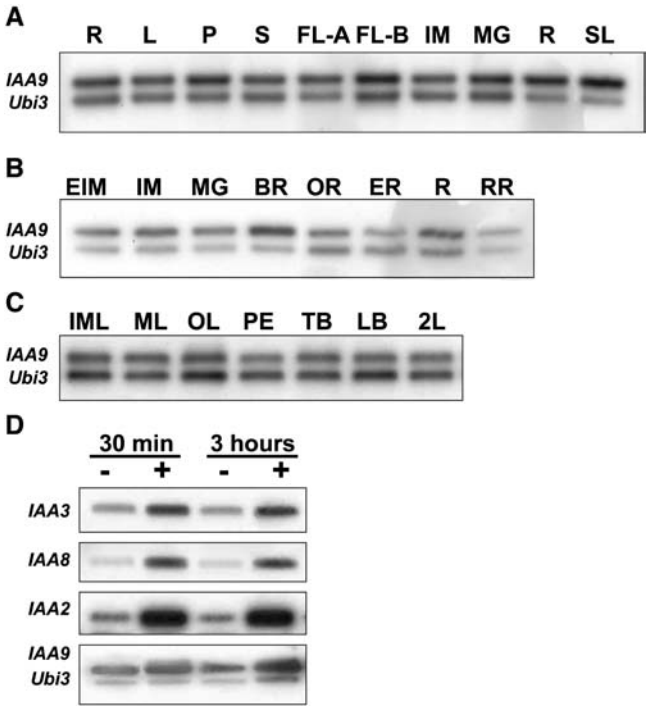

Figure 4. RT-PCR Analysis of *IAA9* Expression Patterns.

(A) *IAA9* expression in different organs: roots (R), leaves (L), petiole (P), stem (S), flowers at anthesis (FL-A), flower buds (FL-B), immature green fruit (IM), mature green fruit (MG), red fruit (R), and seedlings (SL).
(B) *IAA9* expression at different stages of fruit development: early immature green (EIM), immature green (IM), mature green (MG), breaker (BR), orange (OR), early red (ER), red (R), and red ripe (RR).
(C) *IAA9* expression in expanding immature leaves (IML), fully expanded mature leaves (ML), aged, turning yellow leaves (OL), petioles (PE), terminal-leaflet blades (TB), lateral-leaflet blades (LB), and the second leaf counted from the cotyledon node (2L).
(D) Transcript accumulation of *IAA3*, *IAA2*, *IAA8*, and *IAA9* tomato *Aux/IAA* genes in response to auxin treatment (20 μM IAA) of tomato seedlings.

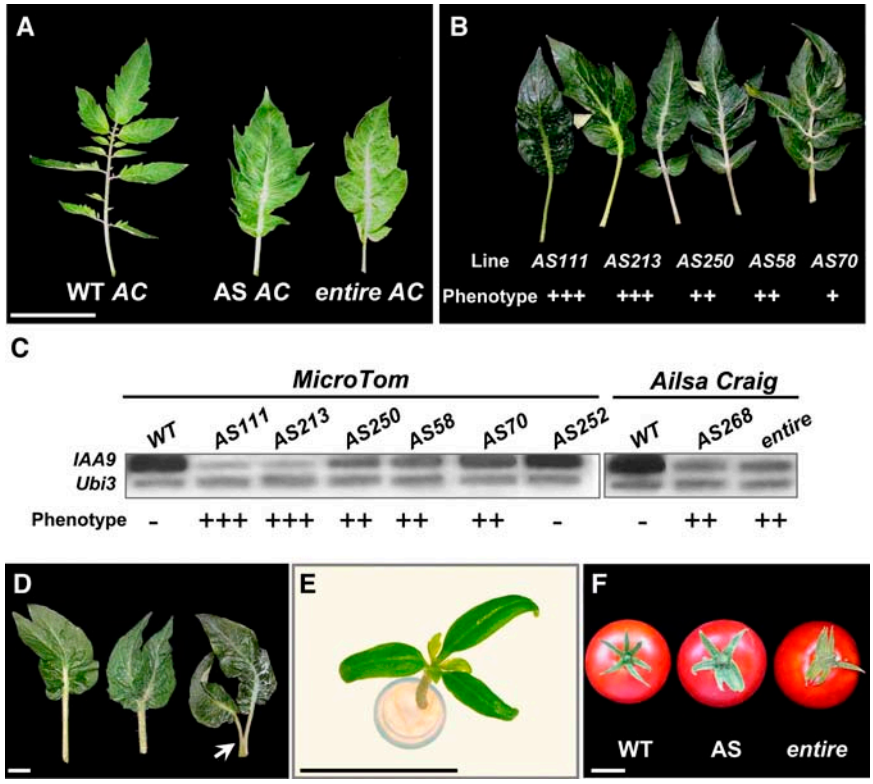

Figure 5. Vegetative Growth Phenotypes of *IAA9* Downregulated Plants.

(A) Tomato leaf morphology in wild-type *Ailsa Craig* (WT *AC*), *IAA9* antisense (AS *AC*), and monogenic spontaneous mutant *entire* (*entire AC*) lines. Bar = 100 mm.

(B) Positive correlation between the severity of the simple-leaf phenotype and the level of downregulation of the *IAA9* gene in *MicroTom* genotype. *AS111* and *AS213* are strongly inhibited lines, and *AS250*, *AS58*, and *AS70* are weakly inhibited lines.

(C) RT-PCR analysis of *IAA9* transcript accumulation in wild-type and antisense lines either in *MicroTom* (*AS111*, *AS213*, *AS250*, *AS58*, *AS70*, and *AS252*) or *Ailsa Craig* (*AS268*) genetic backgrounds and in *entire* mutant plants. Symbols indicate the presence (+) or absence (−) of leaf and parthenocarpy phenotypes. +++ designates lines with only simple leaves and a high percentage of parthenocarpy (60 to 100%); ++ designates lines showing both lobed and entire margin simple leaves and moderate percentage of parthenocarpy (30 to 40%); + designates lines displaying only lobed simple leaves and occasional parthenocarpy.

(D) Leaf fusion in *IAA9* antisense lines consists of either fused twin leaves appearing as a single leaf with two terminal apexes (left), one petiole bearing two lamina (medium), or two leaves partially fused at the end of the petiole and forming a *pin-like* structure (right) as indicated by the arrowhead.

(E) Three-cotyledon structure often occurring in seedlings of strongly inhibited lines.

(F) Fused sepals in antisense lines. Wild-type fruit bear symmetrically arranged calyx, and *AS-IAA9* (AS) and *entire* plants exhibit asymmetrical and partly fused calyx. Bars = 20 mm in **(D)** to **(F)**.

level of downregulation of the *IAA9* gene strongly correlated with the severity of the phenotypes. The most strongly downregulated lines exhibited the highest percentage of parthenocarpic fruit (Figure 6D).

Emasculation assays were performed to determine whether fruit set was independent of pollination and fertilization. Without pollination, fruit set never occurred in emasculated wild-type flowers, while *AS-IAA9* plants developed fruits from the emasculated, unfertilized flowers in all four independent lines tested (Table 1). These fruit proved to be seedless in all cases. The percentage of fruit set from *AS-IAA9* emasculated flowers ranged from 48 to 68% (Table 1) among the four independent transgenic lines. These data indicated that fruit set in *AS-IAA9* lines can occur independently of pollination and fertilization. Cross-pollination assays were performed to examine whether pollen or ovule sterility contributed to the parthenocarpy of *AS-IAA9* lines. Flowers were emasculated before dehiscence of the anthers (pre-anthesis) and manually pollinated. A high percentage of successful fruit set was achieved (79%) using wild-type flowers as the female recipient and *AS-IAA9* plants as the pollen donor. Moreover, all the developed fruits were seeded, and when germinated, all these seeds were kanamycin resistant (Table 2), indicating that *AS-IAA9* pollen were viable. When the reciprocal cross was made, 54% of the pollinated *AS-IAA9* flowers set fruit, and among these, 35% were seeded (Table 2), indicating that the ovules of *AS-IAA9* plants were also fertile. These data clearly indicate that parthenocarpy in *AS-IAA9* lines was mainly due to an alteration of the normal fruit set program.

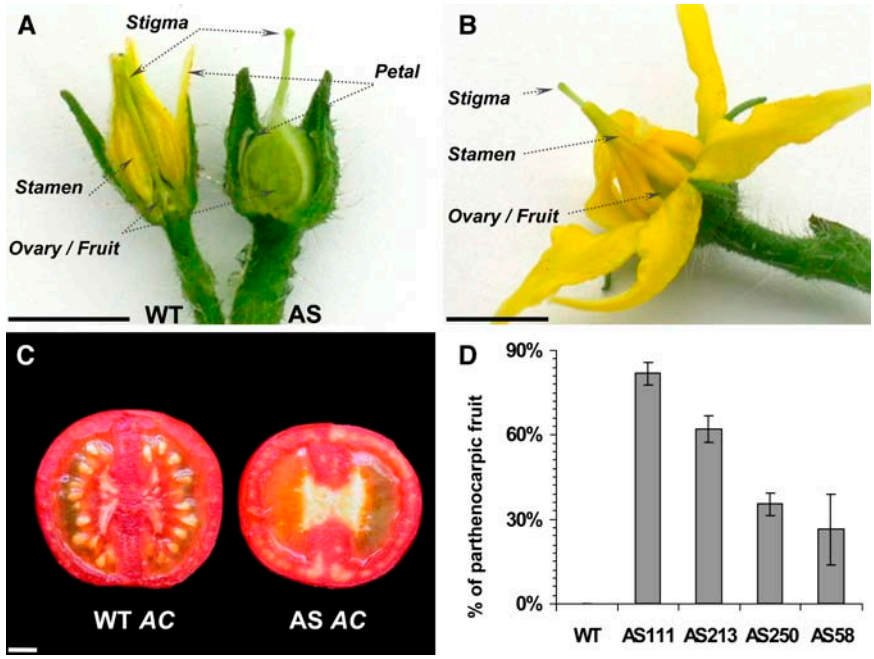

Figure 6. Fruit Set and Parthenocarpy in *AS-IAA9* Lines.

(A) Flower buds at 1 d before anthesis in wild-type and *AS-IAA9* lines (AS), showing dramatically enlarged ovary and underdeveloped stamen in *AS-IAA9* lines.
(B) Precocious fruit development in *AS-IAA9*.
(C) Wild-type *Ailsa Craig* seeded fruit (WT *AC*) and *AS-IAA9* parthenocarpic fruit (AS *AC*). Bars = 10 mm in **(A)** to **(C)**.
(D) The level of parthenocarpy in *AS-IAA9* tomato lines positively correlates with the level of downregulation of the *IAA9* gene in independent *AS-IAA9* lines. Error bars indicate mean ± SE of at least five independent trials, $n \geq 200$ fruits.

AS-IAA9 Plants Showed Increased Stem Elongation and Reduced Apical Dominance

AS-IAA9 plants were usually taller than wild-type plants (Figure 7A) and exhibited enhanced hypocotyl elongation and longer internodes (Figure 7B). *AS-IAA9* plants showed a strongly reduced apical dominance and a dramatically altered pattern of axillary shoot development (Figure 7C). In wild-type tomato plants, lateral shoots appeared only after floral transition and grew out in an apical-basal sequence along the primary shoot axis. In this basipetal growth pattern, the first lateral shoot arises from the last leaf node just below the first inflorescence (Figure 7C). By contrast, *AS-IAA9* plants showed an acropetal growth pattern where the lateral shoots grew out in a basal-apical sequence, the first lateral shoot arising from the first leaf node just above the cotyledon (Figure 7C). As a consequence, in all transgenic lines, lateral shoots were always present in the first three internodes, while in wild-type plants, axillary shoots never arose from the first three internodes (Figure 7D). The level of reduction of apical dominance in the transgenic lines clearly correlated with the level of downregulation of the endogenous *IAA9* gene; that is, the strongly inhibited line *AS213* showed higher apical dominance than the weakly inhibited line *AS250* (Figure 7E). Downregulation of *IAA9* also promoted lateral shoot elongation, resulting in axillary shoots fourfold to fivefold longer than those in control wild-type plants (Figure 7F).

Downregulation of *IAA9* Resulted in Enhanced Auxin Sensitivity

A number of phenotypes associated with the downregulation of *IAA9* suggested enhanced sensitivity to auxin. To further investigate this, we examined auxin dose response on both root formation and hypocotyl segment elongation. Figure 8A shows that the promotion of root organ regeneration from cotyledon explants was auxin dose dependent in both wild-type and *AS-IAA9* plants. However, in wild-type seedlings, the synthetic auxin, α-naphthalene acetic acid (NAA), promoted root regeneration at concentrations above 0.1 μM, while in *AS-IAA9*, the

Table 1. Emasculation Assay to Assess the Ability to Set Fruit in the Absence of Pollination

Lines	Fruit Set (%)	Fruit Set/Emasculated Flower	Seed Number/Fruit
Wild type	0	0/100	0
AS111	63	28/44	0
AS213	68	39/56	0
AS250	49	9/17	0
AS58	48	7/14	0

Wild-type and *AS-IAA9* flowers were emasculated 1 to 4 d before anthesis. The results represent two independent trials.

Table 2. Cross-Fertilization Assay

Female Recipient	Pollen Donor	Fruit Set/Crossed Flowers	Fruit Set (%)	Seeded Fruit (%)	F1 Kanamycin Resistance (%)
Wild type	*AS-IAA9*	65/82	79	100	100
AS-IAA9	Wild type	20/37	54	35	100
Wild type	Wild type	7/7	100	100	0

Tomato pollen from wild-type flowers was used to fertilize emasculated *AS-IAA9* flowers and then the number of fruit assessed at the ripe stage. Conversely, emasculated wild-type flowers were fertilized with *AS-IAA9* pollen. In the control assay, wild-type emasculated flowers were fertilized with wild-type pollen. For each cross-fertilization assay, the proportion of seeded fruit was determined and the capacity of the F1 seeds to grow on kanamycin-containing (70 mg L^{-1}) medium was assessed. The results are representative of data obtained with three independent *AS-IAA9* lines (*AS213*, *AS111*, and *AS250*).

critical concentration was 10-fold lower (0.01 μM). At concentrations higher than optimal, auxin still promoted root formation but inhibited root outgrowth, resulting in short and swollen roots. At 40 μM, root regeneration was almost completely suppressed in *AS-IAA9*, while it was still active in the wild type, indicating that *AS-IAA9* lines were more sensitive to the inhibitory effect of high auxin concentrations. The higher sensitivity of *AS-IAA9* plants to auxin was further explored by determining the auxin dose response on hypocotyl segments. Figure 8B shows that after 23 h of auxin treatment the maximum hypocotyl elongation was obtained with 10^{-4} M for the wild type, while it was reached with a 10-fold lower concentration (10^{-5} M) in the *AS-IAA9* lines.

N-1-Napthylphthalamic Acid–Treated Wild-type Plants Mimicked the Simple-Leaf Phenotype of *AS-IAA9* Plants

Under normal growth conditions, 19-d-old wild-type seedlings had one pair of either compound or deeply lobed leaves and a well-developed primary root bearing one or two lateral roots (Figures 9A and 9C). *AS-IAA9* seedlings grown under the same condition exhibited simple leaves, enhanced primary root elongation (147% longer than the wild type), and an increased number of lateral roots (Figures 9A to 9C). *N*-1-napthylphthalamic acid (NPA), an auxin transport inhibitor, is known to alter the endogenous auxin gradients, resulting in overaccumulation of auxin in root and shoot apices. In wild-type plants, NPA led to the swelling and dramatic reduction of primary root elongation as well as the suppression of lateral root formation. By contrast, primary root growth continued in NPA-treated *AS-IAA9* plants, although lateral root formation was completely inhibited (Figures 9A to 9C). Leaves of wild-type seedlings treated with 1 μM NPA shifted from compound to simple, with an entire leaf margin mimicking the phenotype of *IAA9*-inhibited plants. In *AS-IAA9* lines, NPA treatment enhanced the antisense-associated phenotype by increasing the frequency of leaf fusion and exaggerating the entire leaf margin. It has been postulated that leaf shape is coupled with vascular patterning. We therefore investigated leaf venation in wild-type and antisense plants. Figure 9D shows vein patterning in wild-type, *AS-IAA9*, and NPA-treated leaves. Wild-type leaves had compound unipinnate venation showing discrete vein size orders; the large primary vein or midvein was continuous with the stem vascular bundles and extended along the length of the leaf. Secondary veins branched from the primary vein and extended to the tips of the separate leaflets, which reflected the compound lamina morphogenesis. Tertiary and quaternary veins interconnected veins of higher orders or formed open ends (Figure 9D, left panels). *AS-IAA9* leaves had unipinnate venation but no separate leaflets. The number of secondary veins was increased from six to nine per terminal lamina half in the wild type to 10 to 13 per lamina half in *AS-IAA9* (Figure 9D, middle panels). Moreover, *AS-IAA9* leaves had more tertiary and quaternary veins connecting higher order veins than the wild type, and the number of parallel vascular strands in the midvein and petiole was increased. NPA-treated wild-type plants also displayed a shift from compound to simple unipinnate venation with a dramatic increase of vein branching (Figure 9D, right panels). Compared with *AS-IAA9* lines, the vascular differentiation of NPA-treated wild-type leaves was more dramatic with the leaf tip displaying the most extensive density of disorganized vein strands, resulting in a complete loss of the central vein order. The central regions and petioles of NPA-treated leaves were broadened, and the lamina surface of these hypervascularized leaves was extensively wrinkled (shown in inset of Figure 9A).

IAA9 Selectively Controls the Expression of *IAA3*

Given the strong auxin-associated phenotypes in the *AS-IAA9* lines, we investigated the effect of downregulation of the *IAA9* gene on the expression of a number of early/primary auxin-responsive genes. Figure 10A indicates that basal accumulation of *IAA3* transcripts in roots was higher in *AS-IAA9* than in the wild type. Nevertheless, *IAA3* retained the capacity to respond to exogenous auxin treatment in the *AS-IAA9* genetic background (Figure 10A). By contrast, downregulation of *IAA9* did not alter the basal expression of other auxin-inducible genes, such as *IAA2*, *IAA6*, *SAUR*, and *GH3*, whose transcript accumulation remained identical to that in the wild type and displayed similar auxin inducibility. Since *IAA9* transcript accumulation is reduced in the *entire* mutant, we investigated whether the expression of some other *Aux/IAA* genes was also affected in this mutant. Semiquantitative analyses by RT-PCR indicated that, with the exception of *IAA9*, none of the other eight *Aux/IAA* genes tested showed significantly altered expression in *entire* leaves (see Supplemental Figure 5 online).

To further investigate the role of *IAA9* in controlling the expression of *IAA3*, we examined the expression of a β-glucuronidase (*GUS*) reporter gene driven by the *IAA3* promoter (Pro_{IAA3}) in both wild-type and *AS-IAA9* genetic backgrounds. *IAA3* is a tomato *Aux/IAA* gene that showed rapid induction by auxin (Figure 10A).

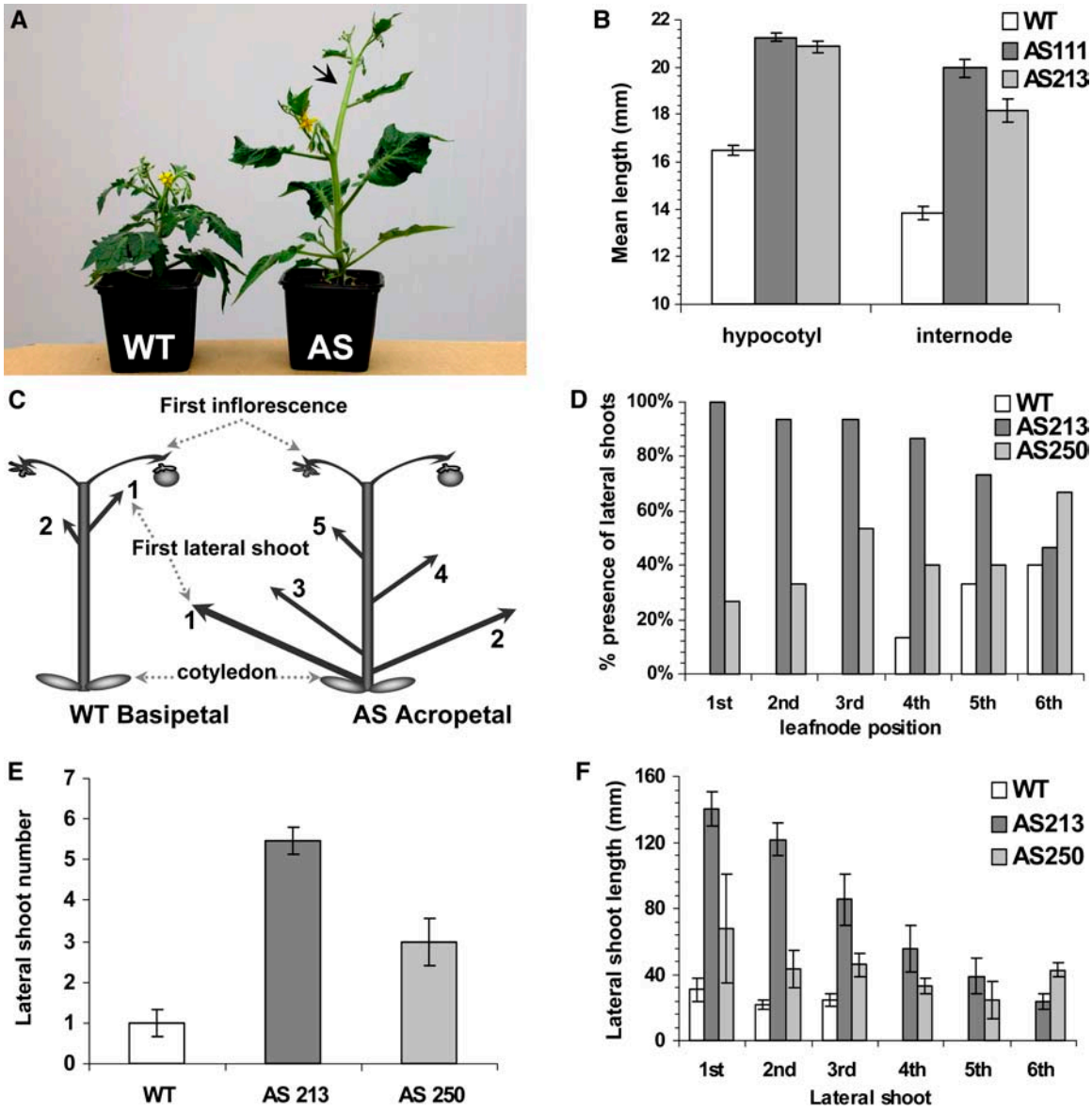

Figure 7. Increased Stem Elongation and Decreased Apical Dominance in *AS-IAA9* Lines.

(A) *AS-IAA9* plants (AS) are taller than the wild type and have longer internodes (indicated by arrow).

(B) Increased hypocotyl and stem elongation in *IAA9* downregulated lines. The data show the hypocotyl mean length of 21-d-old seedlings and internode mean length of 50-d-old plants in wild-type and two independent *AS-IAA9* lines in *MicroTom* genetic background (*AS213* and *AS111*). The data are the mean ± SE of at least 68 seedlings or plants and are representative of three independent experiments.

(C) Diagram depicting the inverted pattern of axillary shoot development and reduced apical dominance in *AS-IAA9* (AS) compared with wild-type plants. Numbers indicate the emergence order of lateral shoots.

(D) Percentage of plants displaying a lateral shoot in each of the first six leaf nodes in wild-type and two antisense lines.

(E) Increased total number of lateral shoots in *AS-IAA9* lines.

(F) *AS-IAA9* lines bear longer lateral shoots. Error bars represent mean ± SE of at least 15 plants in **(E)** and **(F)**.

In the wild-type background, Pro_{IAA3}-driven *GUS* expression was mainly found in the aerial part of the plantlets, particularly in the shoot apex and in the vascular system (Figure 10B), but was barely detectable in the hypocotyl and in the root system, where GUS staining was restricted to small spots corresponding to root tips and lateral root initiation sites (inset of Figure 10B). Upon exogenous auxin treatment, GUS expression in the wild-type background was dramatically increased and spread to all parts of the plantlet (Figure 10C), clearly demonstrating the responsiveness of the *IAA3* promoter to auxin treatment. In *AS-IAA9*

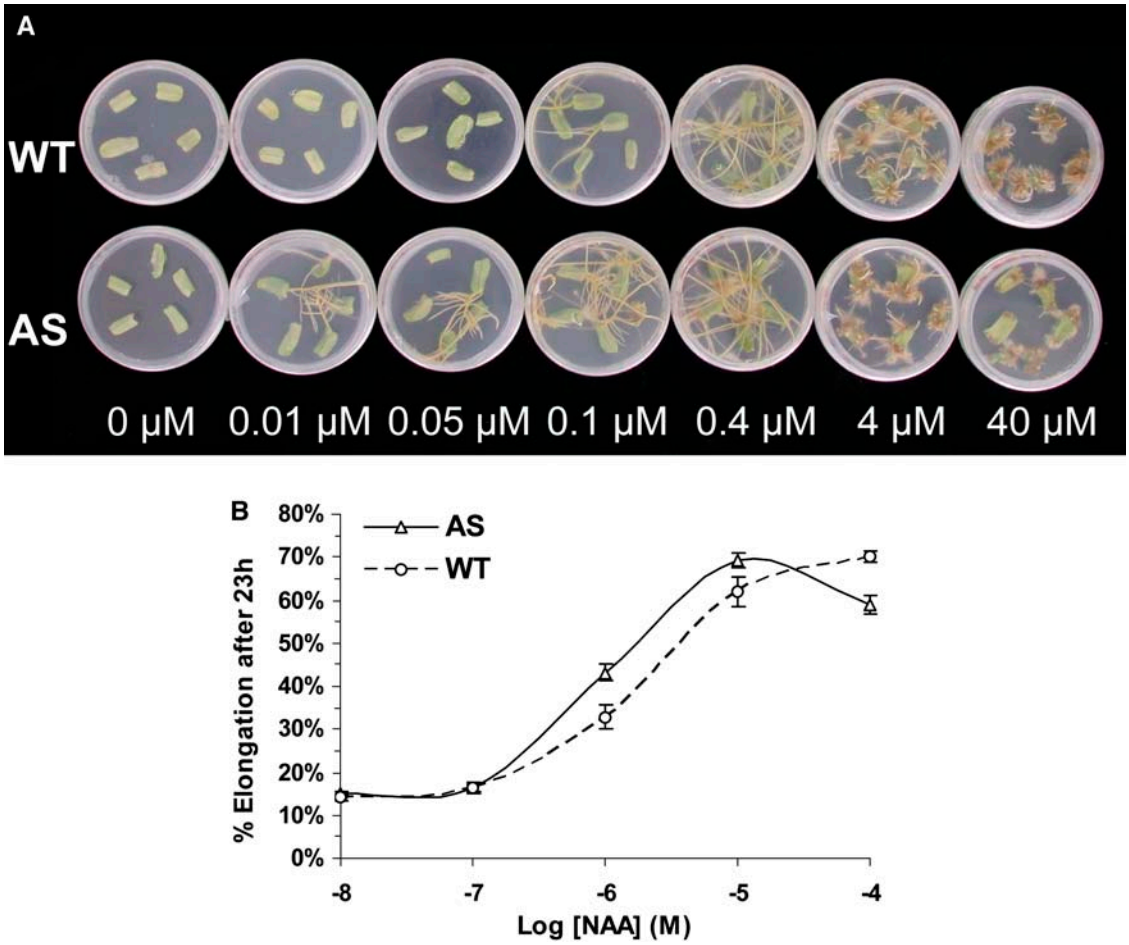

Figure 8. Enhanced Auxin Sensitivity in *IAA9*-Inhibited Lines.

(A) Auxin dose–response assay of cotyledon explants. Root formation is induced by lower auxin (NAA) concentration in *AS-IAA9* (AS) plants than in the wild type. Root regeneration is promoted at 0.1 μM NAA in the wild type and at 10 times lower concentration (0.01 μM) in *AS-IAA9* lines.
(B) Auxin dose response in hypocotyl segments. Elongation is given as percentage increase in final length over the initial length after 23 h incubation in a solution containing the indicated NAA concentration. The results are representative of data obtained with three independent *AS-IAA9* lines: *AS213*, *AS111*, and *AS250*. Error bars represent mean ± SE, $n \geq 20$.

background, Pro_{IAA3} activity was dramatically enhanced in the absence of auxin treatment and displayed a pattern of expression mimicking that of auxin-treated wild-type lines. In particular, the GUS staining was detected over the entire root system, indicating that downregulation of *IAA9* expression induces a constitutive activation of the auxin-responsive promoter and that IAA9 acts as a transcriptional repressor of auxin-induced gene expression.

DISCUSSION

Our understanding of the functional role of Aux/IAA proteins has come mainly through the study of dominant or semidominant, gain-of-function *aux/iaa Arabidopsis* mutant lines. This work reports on the downregulation of a tomato *Aux/IAA* gene, *IAA9*, resulting in a pleiotropic morphological and developmental phenotype. Downregulation of *IAA9* altered leaf architecture and vascular venation patterning, fruit set and development, apical dominance, and many other aspects of vegetative and reproductive growth in the *AS-IAA9* transgenic lines. The pleiotropic phenotypes were consistent with the multiorgan pattern of expression of the *IAA9* gene, and most of them are indicative of a role for the encoded protein in auxin responsiveness. The combined evidence suggests that IAA9 acts as a negative regulator of auxin responses in tomato.

A number of Aux/IAA proteins have been shown to function as transcriptional repressors through interactions with ARF proteins that bind to auxin-responsive elements in the promoters of auxin-responsive genes. In *Arabidopsis*, mutations in domain II of Aux/IAA proteins result in the relative stabilization of the mutated proteins, leading in most cases to phenotypes consistent with a reduced auxin responsiveness (Reed, 2001). Gain-of-function mutations in individual *Arabidopsis Aux/IAA* genes result in distinctive phenotypes, presumably indicative of the specific expression patterns and/or alterations in the dynamics of

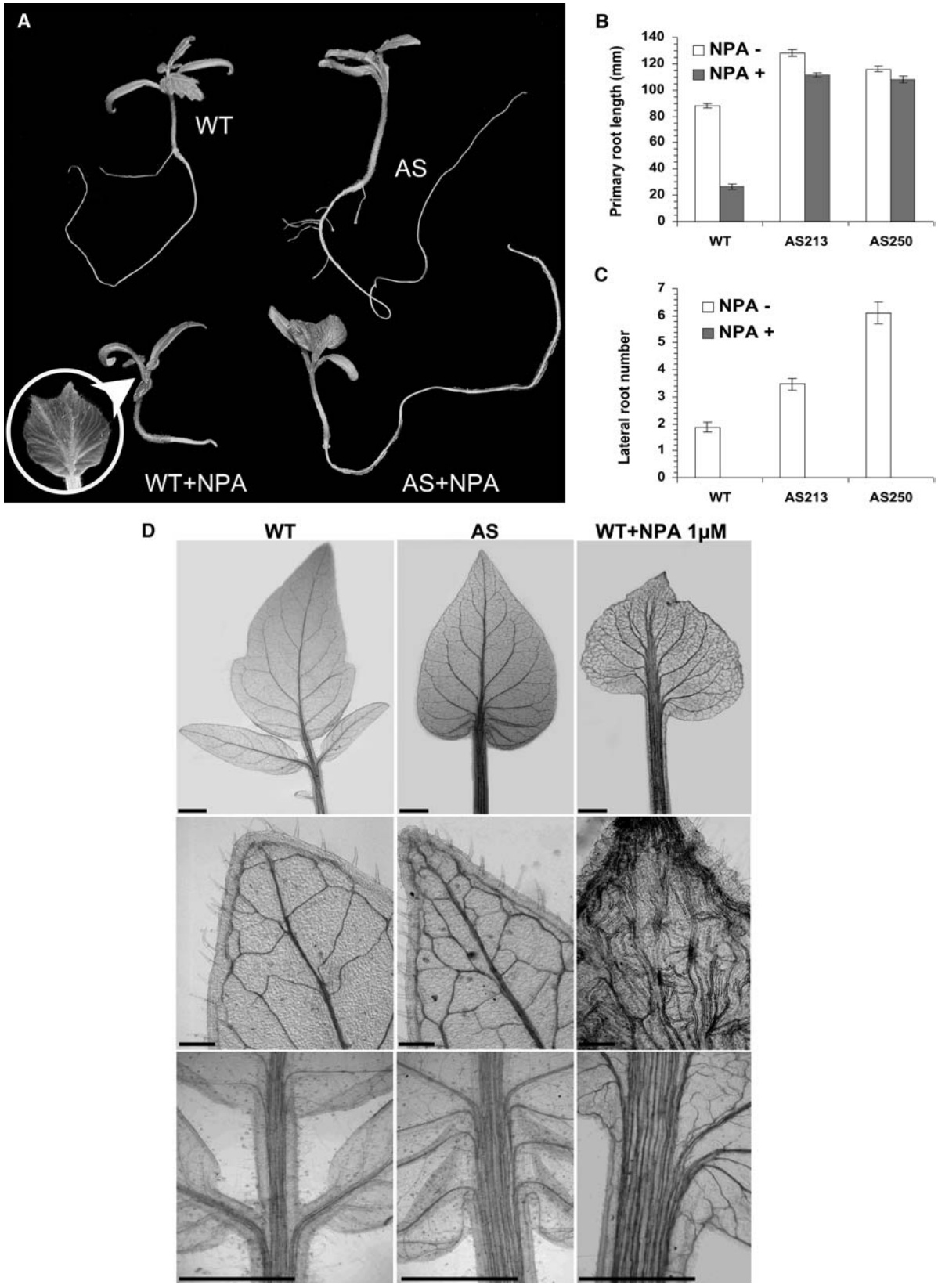

Figure 9. NPA-Treated Wild-Type Plants Phenocopy the Simple-Leaf Phenotype of *AS-IAA9* Plants.

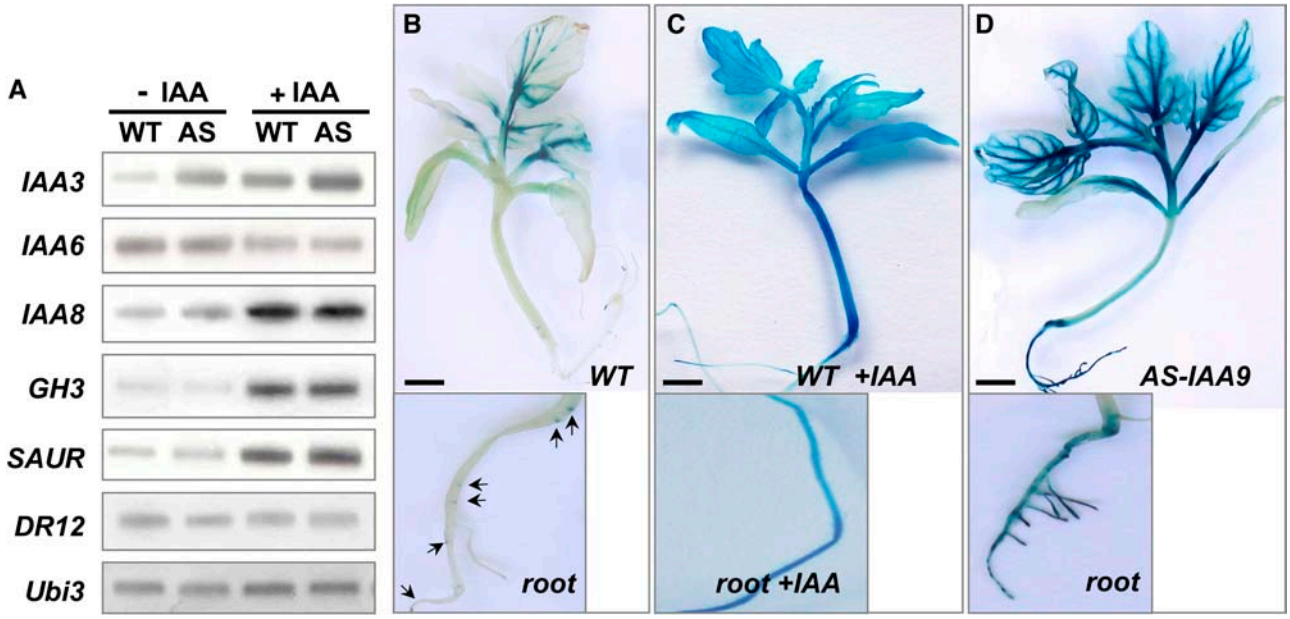

Figure 10. Expression of Primary Auxin-Responsive Genes in *IAA9*-Inhibited Lines.

(A) RT-PCR analyses of the expression of auxin-responsive genes (*IAA3*, *IAA6*, *IAA2*, *GH3*, *SAUR*, and *DR12*) in the wild type and *IAA9*-inhibited (AS) line (*AS213*) upon auxin treatment (20 μM IAA for 3 h).
(B) Expression pattern of the auxin-inducible *IAA3* promoter (Pro_{IAA3}) fused to the *GUS* reporter gene in wild-type seedlings. Inset contains enlarged picture showing GUS staining limited to small spots corresponding to the root tip and lateral root initiation sites (arrowheads).
(C) Expression pattern of Pro_{IAA3}:*GUS* in wild-type seedlings treated with exogenous auxin (20 μM IAA). Inset shows GUS staining throughout the root.
(D) Expression pattern of Pro_{IAA3}:*GUS* in *AS-IAA9* background with no auxin treatment. Inset shows GUS staining present in all parts of the root system.
Bars = 5 mm in **(B)** to **(D)**.

homoprotein/heteroprotein interactions between Aux/IAA and ARFs. Intragenic suppressors of gain-of-function alleles (Timpte et al., 1994; Rouse et al., 1998; Tian and Reed, 1999) and T-DNA insertional mutants (Nagpal et al., 2000) have subtle or indiscernible phenotypes (Reed, 2001; Liscum and Reed, 2002). It is generally thought that functional redundancy in the *Aux/IAA* gene family in *Arabidopsis* accounts for the absence of clear phenotypes, and as an attempt to overcome this problem, efforts are now underway to isolate lines with mutations in several *Aux/IAA*s. In this work, the *IAA9* antisense construct was mainly targeted to the 3′ untranslated region to prevent cross-inhibition of other *Aux/IAA* genes through a sequence homology-based posttranscriptional mechanism. The efficiency of this strategy was validated by assessing the expression of nine *Aux/IAA* genes, including *IAA6*, which shares the highest sequence similarity with *IAA9*, and none of them were downregulated in the *AS-IAA9* transgenic plants (Figure 10A; see Supplemental Figure 5 online). These data support the hypothesis that the observed phenotypes were directly attributable to the downregulation of the *IAA9* gene. Although the phylogenetic data clearly indicate that IAA9 protein bears specific domains that are not found in other Aux/IAA subfamilies, it remains possible, however, that the expression of a yet unidentified tomato *Aux/IAA* might be directly affected by the transgene. We have generated a number of transgenic lines downregulated in other *Aux/IAA* genes, and none of them have reproduced the dramatic leaf and fruit phenotypes displayed by the *AS-IAA9* lines. In this context, the *AS-IAA9* tomato lines present a valuable means to determine Aux/IAA dynamics in auxin response and to reveal distinct roles for *Aux/IAA* genes that have not been described previously, including their role in fruit set and leaf morphogenesis.

Figure 9. (continued).

(A) Mock treatments are presented in the top row, and NPA treatments (1 μM) are presented in the bottom row. NPA-treated wild-type seedlings reproduced the simple-leaf and leaf-fusion phenotypes (inset).
(B) Effect of NPA treatment on primary root elongation in light-grown wild-type and *AS-IAA9* plants.
(C) Inhibition of lateral root formation in wild-type and *AS-IAA9* lines (*AS213* and *AS250*) upon NPA application. Error bars represent mean ± SE ($n \geq 63$).
(D) Leaf vascular patterns in wild-type (left panels), *AS-IAA9* (middle panels), and NPA-treated wild-type plants (right panels). Top row, overall views of venation pattern; middle row, close-up pictures of the leaf tips; bottom row, proximal region of midvein. Bars = 1 mm (top and bottom rows) and 100 μm (middle row).

IAA9 was isolated from a tomato fruit cDNA library and found to code for a putative member of the Aux/IAA protein family (Jones et al., 2002). The strong sequence similarity of the highly conserved Aux/IAA domains I to IV, the nuclear localization of the encoded protein, and the phenotypes of the *AS-IAA9* tomato lines strongly suggest that *IAA9* encodes a functional Aux/IAA protein. *Aux/IAA* multigene families have been isolated from *Arabidopsis* (Abel et al., 1995), tobacco (Dargeviciute et al., 1998), tomato (Nebenfuhr et al., 2000), soybean (*Glycine max*; Ainley et al., 1988), and a number of other dicot and monocot species. Tomato *IAA9* and its putative *Arabidopsis* orthologs, *IAA9* and *IAA8*, belong to *Aux/IAA* subfamily IV (Figure 2), which includes members encoding proteins 50 to 89% larger than Aux/IAAs from all other subfamilies. In addition to the domains I to IV common to all Aux/IAAs, subfamily IV proteins have a highly conserved, extended N-terminal region upstream of domain I and between domains I and II, comprising up to 150 extra amino acids. This includes a $(Pxx)_2$ motif located between domains I and II and several other amino acid domains perfectly conserved across plant species (shaded in gray in Figure 1) that are indicative of a conserved function for these regions.

Auxin responsiveness of *Aux/IAA* genes differs considerably from gene to gene. Depending on the gene and concentration of the exogenous hormone, responses range from strong and rapid induction (Abel et al., 1995) to a slight decrease in transcript abundance (Rogg et al., 2001). *IAA9* exhibits several features in common with its *Arabidopsis* orthologs *IAA9* and *IAA8*, including widespread high-level basal expression compared with other *Aux/IAA* genes and a relatively weak auxin inducibility. No phenotypes have been reported to date for knockout or gain-of-function mutations in any member of subfamily IV in *Arabidopsis* (*IAA9* and *IAA8*) or in any other plant species.

Fruit set is triggered by pollination and fertilization, and auxin signaling is thought to play a dynamic role in the regulation of fruit set and early growth. It has been postulated that auxin is first produced by elongating pollen tubes and then by the embryo and endosperm in the developing seeds. Subsequent development of the fruit appears to depend on these sources of auxin. Supporting this hypothesis, the auxin-resistant tomato mutant, *diageotropica*, has reduced fruit set, fruit weight, and seed production (Balbi and Lomax, 2003) and the application of either auxin or auxin transport inhibitors that cause an increase in auxin in the ovary stimulate fruit set and the development of parthenocarpic fruit (Gustafson, 1937; Beyer and Quebedeaux, 1974). Parthenocarpy has also been induced in tomato, eggplant (*Solanum melongena*), and tobacco by ovary-targeted ectopic expression of *Agrobacterium iaaM* and *rolB* genes, which confer higher auxin production and increased auxin sensitivity, respectively (Ficcadenti et al., 1999; Carmi et al., 2003). Because *AS-IAA9* plants show precocious fruit set and marked parthenocarpy, it appears that in wild-type plants the presence of the IAA9 protein prevents ovary development prior to pollination, potentially by acting as a negative regulator of auxin response pathways. Based on our data supporting a transcriptional repressor activity for IAA9, its downregulation in the antisense lines may release the expression of target auxin-responsive genes, thus mimicking a burst of auxin produced during pollination leading to fruit set and development independent of pollination and fertilization. In the *pat-2* and *pat-3*/*pat-4* tomato mutants, it has been postulated that elevated levels of gibberellins (GAs) account for parthenocarpic fruit set and growth (Fos et al., 2000, 2001). In these mutants, fruit set can be inhibited by paclobutrazol, an inhibitor of GA synthesis, and this inhibition can be reversed by exogenous GA application. Because auxin has been shown to promote GA biosynthesis (Ross et al., 2000) and to modulate GA responses (Fu and Harberd, 2003), it is possible that the precocious fruit set and development in *AS-IAA9* lines is mediated by modified GA responses through auxin/GA crosstalk. Treatment of *AS-IAA9* flowers with paclobutrazol or crosses between *AS-IAA9* lines and GA-deficient mutants (*gib-1*, *gib-2*, and *gib-3*) may reveal whether auxin induces parthenocarpy via GA signaling or whether the two hormones induce fruit set and development by separate, parallel pathways.

Once fruit set has occurred, two peaks of auxin production are seen during normal tomato fruit development (Gillaspy et al., 1993), the first at 10 d after anthesis and the second coinciding with the final phase of seed development. Parthenocarpic fruit are generally smaller than seeded fruit, suggesting that seed-derived auxin is required for full pericarp cell expansion (Mapelli et al., 1978). *AS-IAA9* parthenocarpic fruit are of a similar size to seeded wild-type fruit (Figures 5F and 6C) and have the same flesh consistency and fresh weight, suggesting that downregulation of *IAA9* can also compensate for the lack of seed-influenced pericarp cell expansion.

One of the most striking phenotypes exhibited by the *AS-IAA9* plants is the simple leaf architecture, which stands in a marked contrast to the wild-type compound leaf. In some cases, changes in leaf shape are coupled with changes in vascular patterning, suggesting a link between the controls on cell growth, division, and differentiation (Dengler and Kang, 2001). Although, the molecular mechanisms controlling vascular differentiation and leaf morphogenesis during plant organ ontogeny are yet to be fully elucidated, a number of observations have implicated auxin in the formation of vascular tissues in plant organs. These include vascular strand formation in response to local auxin application (Sachs, 2000) and the effects of impaired auxin transport on vascular patterning (Mattsson et al., 1999; Koizumi et al., 2005). In *Arabidopsis* leaf primordia, auxin response patterns presage sites of procambial differentiation, and auxin is instrumental in patterning *Arabidopsis* leaf vasculature (Mattsson et al., 2003). The *Arabidopsis* gain-of-function *aux/iaa* mutant *bdl* and auxin-resistant mutant *axr6* exhibit severely disrupted vascular networks (Hamann et al., 1999; Hobbie et al., 2000), and in the loss-of-function *arf* mutant, *monopteros*, marginal leaf veins are missing or interrupted (Przemeck et al., 1996). The increased vascular network in *AS-IAA9* leaves indicates that downregulation of *IAA9* resulted in more cells undergoing vascular differentiation and that IAA9 is a key mediator in the auxin-dependent regulation of vascular vein patterning and leaf morphogenesis. Interestingly, treatment of wild-type tomato plants with NPA resulted in a simple leaf shape and enhanced vascular differentiation that mimic the *AS-IAA9* phenotype in an exaggerated manner. It appears, therefore, that in tomato and *Arabidopsis*, disruption of correct pattern of either auxin distribution or response can affect the correct establishment of leaf architecture. Our data bring direct evidence for the role of an *Aux/IAA* gene in leaf morphogenesis and indicate that

enhanced auxin responsiveness leads to altered vascular network patterning and leaf ontogeny. To investigate the possible involvement of IAA9 in other tomato leaf morphology mutants, we examined transcript accumulation of the gene in *entire* and *Lanceolate*, two natural monogenic mutants with a simple-leaf phenotype, and in the *Petroselinum* mutant that has supercompound leaves. *IAA9* transcript accumulation was found to be strongly reduced in the *entire* mutant (Figure 5C) but not in the *Lanceolate* and *Petroselinum* mutants (see Supplemental Figure 1 online). However, in the case of *Lanceolate*, the expression data should be regarded cautiously, as only semidominant mutants are available and the presence of one copy of the wild-type allele may be sufficient to drive a normal expression of the *IAA9* gene. Our data suggest either that LANCEOLATE and PETROSELINUM act downstream of IAA9 or that other signaling pathways not involving IAA9 operate in the making of compound leaves. Ectopic expression of the maize homeobox gene *KNOTTED-1* in tomato resulted in a supercompound leaf architecture, with each leaf having up to 2000 leaflets (Hareven et al., 1996). However, in *AS-IAA9* lines, transcript accumulation of two tomato orthologs of *KNOTTED-1* was not affected in the leaves or in other organs (see Supplemental Figure 2 online). These data suggest the coexistence of multiple components controlling leaf ontogeny and vascular vein system patterning. Moreover, these pathways seem not to compensate for one another, as the presence of all these components seem to be required for proper leaf morphogenesis.

The phenotypes of *AS-IAA9* lines confirm the existence of both overlapping and distinct roles for *Aux/IAA* genes in plant developmental processes. The phenotypes associated with gain-of-function mutations in *Aux/IAA* genes have been attributed in most cases to a reduced auxin responsiveness, and in the *Arabidopsis axr2-1* and *shy2-2* mutants, this was clearly correlated with a lower expression level of some auxin-induced genes (Reed, 2001). Most of the gain-of-function mutants, such as *iaa3/shy2-2*, *iaa6/shy1-1*, *iaa7/axr2-1*, and *iaa17/axr3-1*, have short hypocotyls, and *AS-IAA9* seedlings have longer hypocotyls than the wild type, suggesting that these Aux/IAA proteins may act as inhibitors of hypocotyl elongation. *Arabidopsis* gain-of-function *aux/iaa* mutants display distinct and specific phenotypes. For example, *iaa12/bdl-1* lacks an embryonic root (Hamann et al., 1999), *iaa14/slr* has no lateral roots (Fukaki et al., 2002), and *iaa19/mgs2* mutants have aphototropic hypocotyls (Tatematsu et al., 2004). This not only reveals different roles for the *Aux/IAA* members, but also emphasizes the high level of complexity permitted by the large number of *Aux/IAA* genes. However, it is yet unclear whether these differences result from cell-specific expression or functional differences among the corresponding Aux/IAA proteins. Using an antisense strategy to downregulate other members of the *Aux/IAA* gene family (*IAA1*, *IAA3*, and *IAA8*) in tomato revealed that transgenic lines altered in different gene members share some common phenotypes that related to altered auxin responses, but they also displayed specific, reproducible phenotypes (H. Wang and M. Bouzayen, unpublished data). It is particularly noteworthy that none of these downregulated lines displayed precocious fruit set and parthenocarpy, clearly indicating distinct roles for tomato Aux/IAAs during plant growth and development.

Most of the phenotypes exhibited by *AS-IAA9* plants were consistent with the IAA9 protein being a negative regulator of auxin responses. Expression of the auxin-responsive *IAA3* promoter-driven *GUS* reporter gene in the *AS-IAA9* genetic background clearly indicates that IAA9 can act as a negative regulator of auxin-responsive gene expression. Moreover, the promoter becomes active in tissues and organs where it is normally silent, mimicking the expression pattern obtained upon exogenous auxin treatment.

It is striking that all *Aux/IAA* knockout mutants examined so far have no or subtle phenotypes, while partially silenced *AS-IAA9* lines exhibited clear phenotypes. It is possible that the complete knockout of these genes triggers a compensation mechanism through functionally redundant genes and that this mechanism is not activated when a residual expression of the gene is still present, like in the *AS-IAA9* lines. Strikingly, while a number of *aux/iaa* gain-of-function mutants have been described, our attempts to generate *IAA9*-overexpressing lines under the control of the 35S constitutive promoter were unsuccessful. It is possible that the presence of high levels of IAA9 protein without discrimination between tissue types is incompatible with organ differentiation that is vital to normal plant development. Indeed, in the case of *Arabidopsis aux/iaa* gain-of-function mutants, although the proteins are more stable, the expression of the gene is still under the tight control of the endogenous promoter that continues to finely tune the expression of the mutated gene in a tissue-specific manner. These observations sustain the idea that the expression of *Aux/IAA* genes is under a complex and highly coordinated control mechanism.

METHODS

Plant Material and Growth Conditions

Tomato (*Solanum lycopersicum* Mill. cv *MicroTom* and *Ailsa Craig*) plants were grown under standard greenhouse conditions. The conditions for the culture chamber room are as follows: 14-h-day/10-h-night cycle, 25/20°C day/night temperature, 80% humidity, 250 $\mu mol \cdot m^{-2} \cdot s^{-1}$ intense luminosity. Seeds were first surface-sterilized in 50% bleach solution for 10 min, rinsed seven to nine times in sterile distilled water, and dried on Whatman paper and then sown in recipient Magenta vessels containing 50 mL of 50% Murashige and Skoog (MS) culture medium added with R_3 vitamin (0.5 mg L^{-1} thiamine, 0.25 mg L^{-1} nicotinic acid, and 0.5 mg L^{-1} pyridoxine), 1.5% (w/v) sucrose, and 0.8% (w/v) agar, pH 5.9. The tomato mutants, *entire* LA2922, *Lanceolate* LA335, and *Petroselinum* LA2532, were provided by C.M. Rick Tomato Genetics Resource Center (http://tgrc.ucdavis.edu/).

Plant Transformation

To generate *AS-IAA9* transgenic plants, forward 5′-TGGCCACCCATTC-GATCTTTTAG-3′ and reverse 5′-AGACAAACTCCAATATCAAACGG-3′ primers encompassing the 3′ untranslated region and part of the 3′ terminal coding region of the *IAA9* cDNA were used to amplify a partial *IAA9* clone. This fragment was then cloned into pGA643 binary vector in antisense orientation under the transcriptional control of the cauliflower mosaic virus *35S* promoter and the *Nos* terminator. Transgenic plants were generated by *Agrobacterium tumefaciens*–mediated transformation according to Jones et al. (2002), and transformed lines were first selected on kanamycin (70 mg L^{-1}) and then analyzed by both PCR and DNA gel blot analysis to check the presence and the number of T-DNA insertions and to discriminate between different transformation events in the various transgenic lines obtained.

Phenotypical and Physiological Characterizations of *AS-IAA9*

Phenotypical characterization was performed on homozygote lines. For auxin dose–response experiments, cotyledon explants from wild-type and *AS-IAA9* 9-d-old seedlings were incubated on MS medium containing the indicated auxin (NAA) concentrations in growth chamber conditions described as above for 10 d. For auxin dose–response experiments performed with hypocotyl segments, hypocotyl fragments, 8 mm long, were isolated just below the cotyledons nodes from 5-d-old light-grown seedlings and then immediately floated in sucrose/MES buffer (1% sucrose [w/v] and 5 mM MES/KOH, pH 6.0) in 8-cm Petri dishes. After 1 to 2 h pre-incubation, the hypocotyl segments were randomly distributed to fresh buffer solutions with or without NAA and measured following 23 h of incubation with gentle agitation at room temperature. For NPA treatment, the seeds were sown on MS medium containing 1 μM NPA, and the phenotypes affecting root and leaf growth were observed on young 19-d-old seedlings. For auxin treatment, 21-d-old tomato seedlings were harvested and incubated in 50% MS buffer containing 20 μM IAA or not (mock treatment) for the time indicated (30 min, 3 h). Thereafter, tissues were immediately frozen in liquid nitrogen and stored at −80°C until RNA extraction. For light microscopy used for determination of venation patterning, plant materials were prepared as follows. The third leaves were taken from 28-d-old light-grown seedlings and fixed overnight in a solution (acetic acid 14%, ethanol 84%). The samples were then dehydrated through a graded ethanol series and cleared in a solution of chloral hydrate (200 g chloral hydrate; 20 g glycerol; 50 g distilled water). Stereomicroscopic photographs were taken under light-field conditions. Mature xylem cells appear dark under light-field optics due to the refraction properties of their thicker secondary cell walls.

Flower Emasculation and Cross Assay

Flower buds of wild-type or transgenic plants were emasculated before dehiscence of anthers (closed flowers) to avoid accidental self-pollination. Cross-pollination was performed on emasculated flowers one day prior to anthesis. For emasculation and cross-fertilization experiments, 8 to 10 flowers were kept per plant to ensure equivalent growth conditions for all fruit.

Gene Expression Analysis

Total RNA was extracted according to Jones et al. (2002). The RT-PCR analysis was performed as described previously (Zegzouti et al., 1999), and in each PCR reaction, the internal reference *ubi3* was coamplified with the target gene. Forward (F) and reverse (R) primers used for RT-PCR amplification of the target genes in each RNA sample are the following: for *IAA9* (F 5′-TGGCCACCCATTCGATCTTTTAG-3′ and R 5′-CGCAACACACATTAGTTTGCAG-3′), for *IAA3* (F 5′-AACAAGACTCAGCTCCTGCACC-3′ and R 5′-CATCACCAACAAGCATCCAATC-3′), for *IAA8* (F 5′-ATGACTGAGCTAACTCTCGGCTTA-3′ and R 5′-ACTCGACGATCCCCCAGGTGTTCT-3′), for *IAA2* (F 5′-AAGCGAGCTATGTTAAAGTGAGCA-3′ and R 5′-CCGTTGTATCCATCTGTTTCTGAA-3′), for *IAA6* (F 5′-AGGAGACTGAGCTGAGACTTGGGTT-3′ and R 5′-CAACTTGAACCTGTTCTCCCTTCAT-3′), for *GH3* (F 5′-AGCTCGTCATCACAACATACGC-3′ and R 5′-CAACTCGCCCTTGTCGATAAAC-3′), for *SAUR* (F 5′-GGCTATCCGTATGCCTCGTA and R 5′-CCACCCATCGGATGATTAAA-3′), for *DR12* (F 5′-CATGCTGATTTCGTTGTACCTTAC-3′ and R 5′-GTCTAAAAGAGCACTCCCTC-3′), and for *ubi3* (F 5′-AGAAGAAGACCTACACCAAGCC-3′ and R 5′-TCCCAAGGGTTGTCACATACATC-3′).

Protoplast Isolation and Transient Expression of *IAA9-GFP* Fusion Gene

The coding sequence of *IAA9* was cloned as a C-terminal fusion in frame with the GFP into the pGreen vector (Hellens et al., 2000) and expressed under the control of the *35S* promoter. Protoplasts used for transfection were obtained from suspension-cultured tobacco (*Nicotiana tabacum*) BY-2 cells according to the method described previously (Leclercq et al., 2005). Protoplasts were transfected by a modified polyethylene glycol method as described by Abel and Theologis (1994). Typically, 0.2 mL of protoplast suspension (0.5 × 106) was transfected with 50 μg of shared salmon sperm carrier DNA and 30 μg of either *35S:IAA9-GFP* or *35S:GFP* (control) plasmid DNA. Transfected protoplasts were incubated 16 h at 25°C and analyzed for GFP fluorescence by confocal microscopy as by Leclercq et al. (2005). All transient expression assays were repeated at least three times.

Histochemical GUS Analysis

Transgenic lines bearing the *IAA3* promoter/*GUS* fusion construct (*Pro$_{IAA3}$-GUS*) were incubated at 37°C overnight with GUS staining solution (100 mM sodium phosphate buffer, pH 7.2, 10 mM EDTA, 0.1% Triton, and 1 mM 5-bromo-4-chloro-3-indolyl-β-D-glucuronic acid) to reveal GUS activity. Following GUS staining, samples were washed several times to extract chlorophyll using a graded ethanol series.

Sequence Analysis

Amino acid sequence alignments were performed using ClustalW (http://bioweb.pasteur.fr/seqanal/interfaces/clustalw-simple.html) assisted by manual adjustment. Phylogenetic analyses were performed with PAUP (Phylogenetic Analysis Using Parsimony, version 4.0 b10). All heuristic searches for optimal trees were performed by TBR (tree bisection reconnection) branch swapping with option MULPARS in effect. Starting trees were obtained by random addition (10 replicates). For each of the 5000 bootstrap replicates, 10 heuristic searches were performed with random addition of protein samples. The phylogenetic tree was displayed with TreeView (http://taxonomy.zoology.gla.ac.uk/rod/treeview.html).

Accession Numbers

Sequence data from this article can be found in the GenBank/EMBL data libraries under accession number AJ937282. GenBank accession numbers for the sequences analyzed in the phylogenetic analysis are as follows: AtIAA1 (P49677), AtIAA2 (P49678), AtIAA3 (Q38822), AtIAA4 (P33077), AtIAA5 (P33078), AtIAA6 (Q38824), AtIAA7 (Q38825), AtIAA8 (Q38826), AtIAA9 (Q38827), AtIAA10 (Q38828), AtIAA11 (Q38829), AtIAA12 (Q38830), AtIAA13 (Q38831), AtIAA14 (Q38832), AtIAA16 (O24407), AtIAA17 (P93830), AtIAA18 (O24408), AtIAA19 (O24409), AtIAA20 (O24410), AtIAA26 (Q8LAL2), AtIAA27 (Q9ZSY8), AtIAA28 (Q9XFM0), AtIAA29 (Q93WC4), AtIAA30 (Q9M1R4), AtIAA31 (Q8H174), AtIAA32 (Q8RYC6), AtIAA33 (Q9FKM7), AtIAA34 (Q9C5X0), ZeARP (AAM12952), NtIAA9 (CAD10639), VvIAA (AAL92850), StIAA (AAM29182), CsIAA2 (BAA85821), OsIAAa (BAD81331.1), OsIAAb (BAD67992.1), OsIAAc (BAD22024.1), OsIAA1 (CAC80823.1), OsIAA2 (AAK98708.1), OsIAA8 (CAF28457.1), and OsIAA18 (BAA99424.1).

ACKNOWLEDGMENTS

This work was supported by the Midi-Pyrénées Regional Council (Grants 01008920 and 03001146) and forms part of the requirement for the degree of PhD for H.W. We thank Alain Jauneau for technical support in confocal microscopy analysis, Luc Legal for his helpful advice in performing phylogenetic analysis, and Lydie Tessarotto, Hélène Mondiès, and Dominique Saint-Martin for tomato genetic transformation and plant growth. H.W. was supported by a scholarship from the Association Franco-Chinoise pour la Recherche Scientifique et Technique and Z.L. by a scholarship from the Institut National de la Recherche Agronomique.

Received April 12, 2005; revised June 13, 2005; accepted August 3, 2005; published August 26, 2005.

REFERENCES

Abel, S., Nguyen, M.D., and Theologis, A. (1995). The *PS-IAA4/5*-like family of early auxin-inducible mRNAs in *Arabidopsis thaliana.* J. Mol. Biol. **251,** 533–549.

Abel, S., and Theologis, A. (1994). Transient transformation of *Arabidopsis* leaf protoplasts: A versatile experimental system to study gene expression. Plant J. **5,** 421–427.

Ainley, W.M., Walker, J.C., Nagao, R.T., and Key, J.L. (1988). Sequence and characterization of two auxin-regulated genes from soybean. J. Biol. Chem. **263,** 10658–10666.

Balbi, V., and Lomax, T.L. (2003). Regulation of early tomato fruit development by the *diageotropica* gene. Plant Physiol. **131,** 186–197.

Beyer, E.M., and Quebedeaux, B. (1974). Parthenocarpy in cucumber: Mechanism of action of auxin transport inhibitors. J. Am. Soc. Hortic. Sci. **99,** 385–390.

Carmi, N., Salts, Y., Dedicova, B., Shabtai, S., and Barg, R. (2003). Induction of parthenocarpy in tomato via specific expression of the *rolB* gene in the ovary. Planta **217,** 726–735.

Dargeviciute, A., Roux, C., Decreux, A., Sitbon, F., and Perrot-Rechenmann, C. (1998). Molecular cloning and expression of the early auxin-responsive *Aux/IAA* gene family in *Nicotiana tabacum.* Plant Cell Physiol. **39,** 993–1002.

Dengler, N., and Kang, J. (2001). Vascular patterning and leaf shape. Curr. Opin. Plant Biol. **4,** 50–56.

Dharmasiri, N., Dharmasiri, S., and Estelle, M. (2005). The F-box protein TIR1 is an auxin receptor. Nature **435,** 441–445.

Ficcadenti, N., Sestili, S., Pandolfini, T., Cirillo, C., Rotino, G., and Spena, A. (1999). Genetic engineering of parthenocarpic fruit development in tomato. Mol. Breed. **5,** 463–470.

Fos, M., Nuez, F., and Garcia-Martinez, J.L. (2000). The gene *pat-2*, which induces natural parthenocarpy, alters the gibberellin content in unpollinated tomato ovaries. Plant Physiol. **122,** 471–480.

Fos, M., Proano, K., Nuez, F., and Garcia-Martinez, J.L. (2001). Role of gibberellins in parthenocarpic fruit development induced by the genetic system *pat-3/pat-4* in tomato. Physiol. Plant **111,** 545–550.

Friml, J. (2003). Auxin transport—Shaping the plant. Curr. Opin. Plant Biol. **6,** 7–12.

Fu, X., and Harberd, N.P. (2003). Auxin promotes *Arabidopsis* root growth by modulating gibberellin response. Nature **421,** 740–743.

Fukaki, H., Tameda, S., Masuda, H., and Tasaka, M. (2002). Lateral root formation is blocked by a gain-of-function mutation in the *SOLITARY-ROOT/IAA14* gene of *Arabidopsis.* Plant J. **29,** 153–168.

Galweiler, L., Guan, C., Muller, A., Wisman, E., Mendgen, K., Yephremov, A., and Palme, K. (1998). Regulation of polar auxin transport by AtPIN1 in *Arabidopsis* vascular tissue. Science **282,** 2226–2230.

Gillaspy, G., Ben-David, H., and Gruissem, W. (1993). Fruit: A developmental perspective. Plant Cell **5,** 1439–1451.

Gustafson, F.G. (1937). Parthenocarpy induced by pollen extracts. Am. J. Bot. **24,** 102–107.

Hamann, T., Benkova, E., Baurle, I., Kientz, M., and Jurgens, G. (2002). The *Arabidopsis BODENLOS* gene encodes an auxin response protein inhibiting *MONOPTEROS*-mediated embryo patterning. Genes Dev. **16,** 1610–1615.

Hamann, T., Mayer, U., and Jurgens, G. (1999). The auxin-insensitive *bodenlos* mutation affects primary root formation and apical-basal patterning in the *Arabidopsis* embryo. Development **126,** 1387–1395.

Hareven, D., Gutfinger, T., Parnis, A., Eshed, Y., and Lifschitz, E. (1996). The making of a compound leaf: Genetic manipulation of leaf architecture in tomato. Cell **84,** 735–744.

Hellens, R.P., Edwards, A.E., Leyland, N.R., Bean, S., and Mullineaux, P. (2000). pGreen: A versatile and flexible binary Ti vector for *Agrobacterium*-mediated plant transformation. Plant Mol. Biol. **42,** 819–832.

Hobbie, L., McGovern, M., Hurwitz, L.R., Pierro, A., Liu, N.Y., Bandyopadhyay, A., and Estelle, M. (2000). The *axr6* mutants of *Arabidopsis thaliana* define a gene involved in auxin response and early development. Development **127,** 23–32.

Jones, B., Frasse, P., Olmos, E., Zegzouti, H., Li, Z.G., Latche, A., Pech, J.C., and Bouzayen, M. (2002). Down-regulation of DR12, an auxin-response-factor homolog, in the tomato results in a pleiotropic phenotype including dark green and blotchy ripening fruit. Plant J. **32,** 603–613.

Kepinski, S., and Leyser, O. (2005). The Arabidopsis F-box protein TIR1 is an auxin receptor. Nature **435,** 446–451.

Kessler, S., and Sinha, N. (2004). Shaping up: The genetic control of leaf shape. Curr. Opin. Plant Biol. **7,** 65–72.

Kim, B.C., Soh, M.S., Kang, B.G., Furuya, M., and Nam, H.G. (1996). Two dominant photomorphogenic mutations of *Arabidopsis thaliana* identified as suppressor mutations of *hy2.* Plant J. **15,** 441–456.

Kim, J., Harter, K., and Theologis, A. (1997). Protein-protein interactions among the Aux/IAA proteins. Proc. Natl. Acad. Sci. USA **94,** 11786–11791.

Koizumi, K., Naramoto, S., Sawa, S., Yahara, N., Ueda, T., Nakano, A., Sugiyama, M., and Fukuda, H. (2005). VAN3 ARF-GAP-mediated vesicle transport is involved in leaf vascular network formation. Development **132,** 1699–1711.

Leclercq, J., Ranty, B., Sanchez-Ballesta, M.T., Li, Z., Jones, B., Jauneau, A., Pech, J.C., Latche, A., Ranjeva, R., and Bouzayen, M. (2005). Molecular and biochemical characterization of LeCRK1, a ripening-associated tomato CDPK-related kinase. J. Exp. Bot. **56,** 25–35.

Liscum, E., and Reed, J.W. (2002). Genetics of Aux/IAA and ARF action in plant growth and development. Plant Mol. Biol. **49,** 387–400.

Mapelli, S.C., Frova, G., Torti, G., and Soressi, G. (1978). Relationship between set, development and activities of growth regulators in tomato fruits. Plant Cell Physiol. **19,** 1281–1288.

Mattsson, J., Ckurshumova, W., and Berleth, T. (2003). Auxin signaling in Arabidopsis leaf vascular development. Plant Physiol. **131,** 1327–1339.

Mattsson, J., Sung, Z.R., and Berleth, T. (1999). Responses of plant vascular systems to auxin transport inhibition. Development **126,** 2979–2991.

Nagpal, P., Walker, L.M., Young, J.C., Sonawala, A., Timpte, C., Estelle, M., and Reed, J.W. (2000). *AXR2* encodes a member of the Aux/IAA protein family. Plant Physiol. **123,** 563–574.

Nebenfuhr, A., White, T.J., and Lomax, T.L. (2000). The *diageotropica* mutation alters auxin induction of a subset of the *Aux/IAA* gene family in tomato. Plant Mol. Biol. **44,** 73–84.

Ouellet, F., Overvoorde, P.J., and Theologis, A. (2001). IAA17/AXR3: Biochemical insight into an auxin mutant phenotype. Plant Cell **13,** 829–841.

Park, J.Y., Kim, H.J., and Kim, J. (2002). Mutation in domain II of IAA1 confers diverse auxin-related phenotypes and represses auxin-activated expression of *Aux/IAA* genes in steroid regulator-inducible system. Plant J. **32,** 669–683.

Przemeck, G.K., Mattsson, J., Hardtke, C.S., Sung, Z.R., and Berleth, T. (1996). Studies on the role of the *Arabidopsis* gene *MONOPTEROS* in vascular development and plant cell axialization. Planta **200,** 229–237.

Reed, J.W. (2001). Roles and activities of Aux/IAA proteins in *Arabidopsis.* Trends Plant Sci. **6,** 420–425.

Rogg, L.E., Lasswell, J., and Bartel, B. (2001). A gain-of-function mutation in *IAA28* suppresses lateral root development. Plant Cell **13,** 465–480.

Ross, J.J., O'Neill, D.P., Smith, J.J., Kerckhoffs, L.H., and Elliott, R.C. (2000). Evidence that auxin promotes gibberellin A1 biosynthesis in pea. Plant J. **21,** 547–552.

Rouse, D., Mackay, P., Stirnberg, P., Estelle, M., and Leyser, O. (1998). Changes in auxin response from mutations in an *AUX/IAA* gene. Science **279,** 1371–1373.

Sachs, T. (2000). Integrating cellular and organismic aspects of vascular differentiation. Plant Cell Physiol. **41,** 649–656.

Servant, F., Bru, C., Carrere, S., Courcelle, E., Gouzy, J., Peyruc, D., and Kahn, D. (2002). ProDom: Automated clustering of homologous domains. Brief. Bioinform. **3,** 246–251.

Tatematsu, K., Kumagai, S., Muto, H., Sato, A., Watahiki, M.K., Harper, R.M., Liscum, E., and Yamamoto, K.T. (2004). *MASSUGU2* encodes Aux/IAA19, an auxin-regulated protein that functions together with the transcriptional activator NPH4/ARF7 to regulate differential growth responses of hypocotyl and formation of lateral roots in *Arabidopsis thaliana.* Plant Cell **16,** 379–393.

Tian, Q., and Reed, J.W. (1999). Control of auxin-regulated root development by the *Arabidopsis thaliana SHY2/IAA3* gene. Development **126,** 711–721.

Timpte, C., Wilson, A.K., and Estelle, M. (1994). The *axr2-1* mutation of *Arabidopsis thaliana* is a gain-of-function mutation that disrupts an early step in auxin response. Genetics **138,** 1239–1249.

Tiwari, S.B., Hagen, G., and Guilfoyle, T.J. (2004). Aux/IAA proteins contain a potent transcriptional repression domain. Plant Cell **16,** 533–543.

Ulmasov, T., Hagen, G., and Guilfoyle, T.J. (1997). ARF1, a transcription factor that binds to auxin response elements. Science **276,** 1865–1868.

Vogler, H., and Kuhlemeier, C. (2003). Simple hormones but complex signalling. Curr. Opin. Plant Biol. **6,** 51–56.

Yang, X., Lee, S., So, J.H., Dharmasiri, S., Dharmasiri, N., Ge, L., Jensen, C., Hangarter, R., Hobbie, L., and Estelle, M. (2004). The IAA1 protein is encoded by *AXR5* and is a substrate of SCF^{TIR1}. Plant J. **40,** 772–782.

Zegzouti, H., Jones, B., Frasse, P., Marty, C., Maitre, B., Latch, A., Pech, J.C., and Bouzayen, M. (1999). Ethylene-regulated gene expression in tomato fruit: Characterization of novel ethylene-responsive and ripening-related genes isolated by differential display. Plant J. **18,** 589–600.